1064 nm Deep Near-Infrared (NIR) Excited Raman Microspectroscopy for Studying Photolabile Organisms

MASAHIRO ANDO, MIWA SUGIURA, HIDENORI HAYASHI, and HIRO-O HAMAGUCHI*

Department of Chemistry, School of Science, The University of Tokyo, 7-3-1 Hongo, Bunkyo-ku, Tokyo 113-0033, Japan (M.A., H.H.); Cell-Free Science and Technology Research Center, Ehime University, Bunkyo-cho, Matsuyama Ehime, 790-8577, Japan (M.S., H.H.); and Department of Applied Chemistry, College of Science, National Chiao Tung University, 1001 Ta Hsueh Road, Hsinchu, Taiwan 300, Republic of China (H.H.)

We have constructed a 1064 nm deep near-infrared (NIR) excited multichannel Raman microspectrometer using an InP/InGaAsP multichannel detector. This microspectrometer achieves high sensitivity suitable for in vivo measurements of single living cells with lateral resolution of 0.7 μm and depth resolution of 3.1 μm. It has been applied to the structural analysis of living cyanobacterial cells, well-known model organisms for photosynthesis research, which are too photolabile to be measured with visible laser excitation. High signal-to-noise ratio (S/N) Raman spectra have been obtained from carotenoid, chlorophyll *a*, and phycocyanin in a single living cyanobacterial cell with no appreciable interference from autofluorescence or photodamage. Sub-micrometer mapping of Raman intensities provides clear distribution images of the three pigments inside the cell.

Index Headings: **Near-infrared Raman spectroscopy; Multichannel Raman spectroscopy; 1064 nm excitation; Microspectroscopy; Cyanobacteria; *Thermosynechococcus elongatus*.**

INTRODUCTION

In vivo molecular-level investigation of cellular processes is of great importance in understanding life. Raman microspectroscopy is now well recognized as one of the most informative methods for studying the structure and function of single living cells, providing sub-micrometer space-resolved molecular information without any sample pretreatment.[1–3] However, this method is not readily applicable to photosensitive/photolabile organisms because of the following two difficulties. One is that such organisms often emit strong autofluorescence that easily interferes with the Raman measurements. The other difficulty is that photolabile systems are easily photodamaged by visible excitation. Some photosensitive organisms emit strong fluorescence and/or are photodamaged even with near-infrared (NIR) excitation at ~800 nm.[4–6]

Deep NIR excitation at 1064 nm overcomes these difficulties,[6–19] though it suffers from low efficiencies due to the low Raman scattering cross-section and the low quantum efficiency of detectors. Over the last decade, we have been developing deep NIR Raman spectroscopy using a newly developed InP/InGaAsP multichannel detector for in vivo measurements of human tissues.[6,14–18] In the present study, we extend this method to microspectroscopy for studying photolabile living organisms. In the measurement of living organisms under a microscope, the excitation laser power needs to be reduced as much as possible, preferably to less than 1 mW, in order to avoid photodamage. We then need to achieve much higher sensitivity than that of existing NIR Raman spectrometers. In the present study, this high sensitivity has been achieved with the use of a deep NIR optimized microscope, a simplified confocal optical configuration, and an improved InP/InGaAsP multichannel detector.

This new apparatus has been applied to the structural analysis of single living cyanobacterial cells, which are prototype model organisms for photosynthesis research. Because cyanobacteria contain several kinds of photosynthetic pigments, they emit strong autofluorescence even with ~800 nm excitation. By using 1064 nm deep NIR excitation, it has become possible to obtain high S/N Raman spectra from carotenoid, chlorophyll *a*, and phycocyanin and their distribution images in a single living cyanobacterial cell.

EXPERIMENTAL

Near-Infrared Raman Microspectroscopy. A schematic diagram of our deep NIR multichannel Raman microspectrometer is shown in Fig. 1. A diode-pumped Q-switched Nd:YAG laser (Spectra Physics T40-X30S-106Q, wavelength 1064 nm, repetition rate 10 kHz, pulse duration 30 ns) is used as the deep NIR excitation source. The 1064 nm laser beam is focused onto a sample with an NIR optimized ×100/1.3 NA microscope objective. Raman scattered light is collected by the same objective, passed through two notch filters, and finally focused on the entrance slit of a polychromator (HORIBA Jobin Yvon, iHR320, 150 grooves/mm grating). A 50 × 50 μm cross slit is used as the entrance slit of the polychromator. This cross slit also functions as a confocal pin hole, reducing the number of optics used and increasing the throughput of the Raman collection optics. An InP/InGaAsP near-infrared image intensifier (Hamamatsu Photonics, 26 × 128 pixels, quantum efficiency approximately 4% for 0.9–1.4 μm) is used in combination with a CCD camera (Andor, iDus DU420A-BV). In order to reduce the thermal noise level, the image intensifier is electrically gated with 100 ns width, synchronized with the Nd:YAG laser pulse. The lateral spatial resolution of 0.7 μm and the depth spatial resolution of 3.1 μm are estimated from the signal intensity profile at the edge of a silicon plate and that at the cyclohexane–glass interface, respectively. Approximately 1000 cm^{-1} wavenumber region is simultaneously measured with 10 cm^{-1} spectral resolution.

In order to avoid photodamage of the sample, the laser power is reduced to less than 1 mW at the sample point, typically 0.5 mW. In the measurement of a single point inside the cell, Raman spectra are obtained with an accumulation time of 30 seconds. In the measurements of pigment samples, accumulation time is 5–10 minutes. In the Raman mapping

Received 29 November 2010; accepted 14 January 2011.

* Author to whom correspondence should be sent. E-mail: hhama@chem.s.u-tokyo.ac.jp.

DOI: 10.1366/10-06196

0003-7028/11/6505-0488$2.00/0

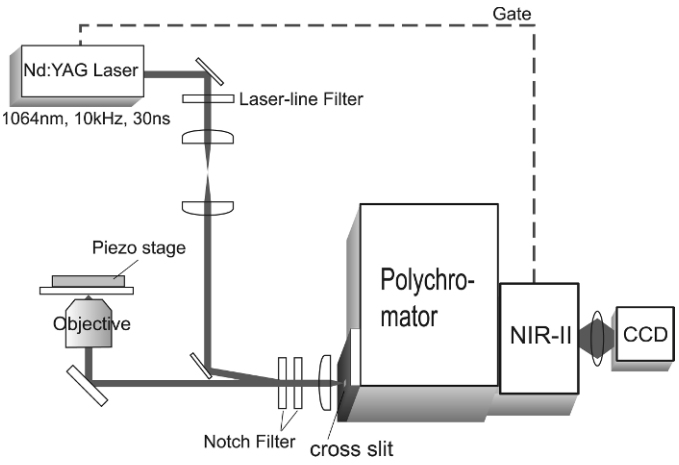

FIG. 1. Schematic diagram of the 1064 nm excited multichannel Raman microspectrometer.

measurement, the sample is translated by a piezoelectric stage (Madcity, Nano-LP-100) horizontally with a step of 0.3 μm. At each sample point, Raman spectra are measured in 10 seconds. In order to increase the signal-to-noise ratio (S/N), a singular value decomposition analysis is performed to remove uncorrelated random noise.[20]

A 785 nm excited confocal Raman microspectrometer is also used in order to examine the effect of excitation wavelength. A tunable Ti:Sapphire laser (Spectra Physics, 3900S, pumped by Millenia Pro, Spectra Physics) set at 785 nm is used as the excitation source. An oil immersion ×100/1.25 NA objective and a 50 μm pinhole are used to achieve the confocal effect. The lateral spatial resolution of 0.4 μm and the depth spatial resolution of 3.5 μm are estimated in the same way as in the 1064 nm excitation system. Spectral resolution is 4 cm^{-1}. Accumulation time is 10s with excitation laser power of 0.6 mW at the sample point.

Sample. The cells of thermophilic cyanobacterium, *Thermosynechococcus elongatus*, were cultivated at 45 °C under light illumination at ~60 μmol of photons·s^{-1}·m^{-2} as previously described.[21] For the preparation of the sample for Raman measurements, *T. elongatus* cells in medium were put between the slide and cover glasses. By controlling the quantity of the medium, the thickness of the sample layer was adjusted close to the diameter of the cells so that they were physically fixed by the two glass plates.

The model compounds, β-carotene, chlorophyll *a*, and C-phycocyanin, were purchased from Sigma-Aldrich (Japan) and used as received (powder) for the Raman measurements.

RESULTS AND DISCUSSION

In order to show the capability of the present deep NIR excited Raman microspectrometer, we compare in Fig. 2 the Raman spectra of *T. elongatus* cells measured with 1064 nm and 785 nm excitation. With 785 nm NIR excitation, fluorescence from photosynthetic pigments strongly interferes and Raman bands are barely seen on a high background. It is also seen that the profile of the fluorescence background changes with time. This finding indicates that, even with 785 nm NIR excitation, the laser irradiation perturbs the *T. elongatus* cellular processes and causes photodamage. On the other hand, 1064 nm deep NIR excitation drastically decreases the autofluorescence and shows several clear Raman bands. Furthermore, the spectra do not show time dependence, indicating that the photodamage or photobleaching does not occur. It is thus demonstrated that the present deep NIR

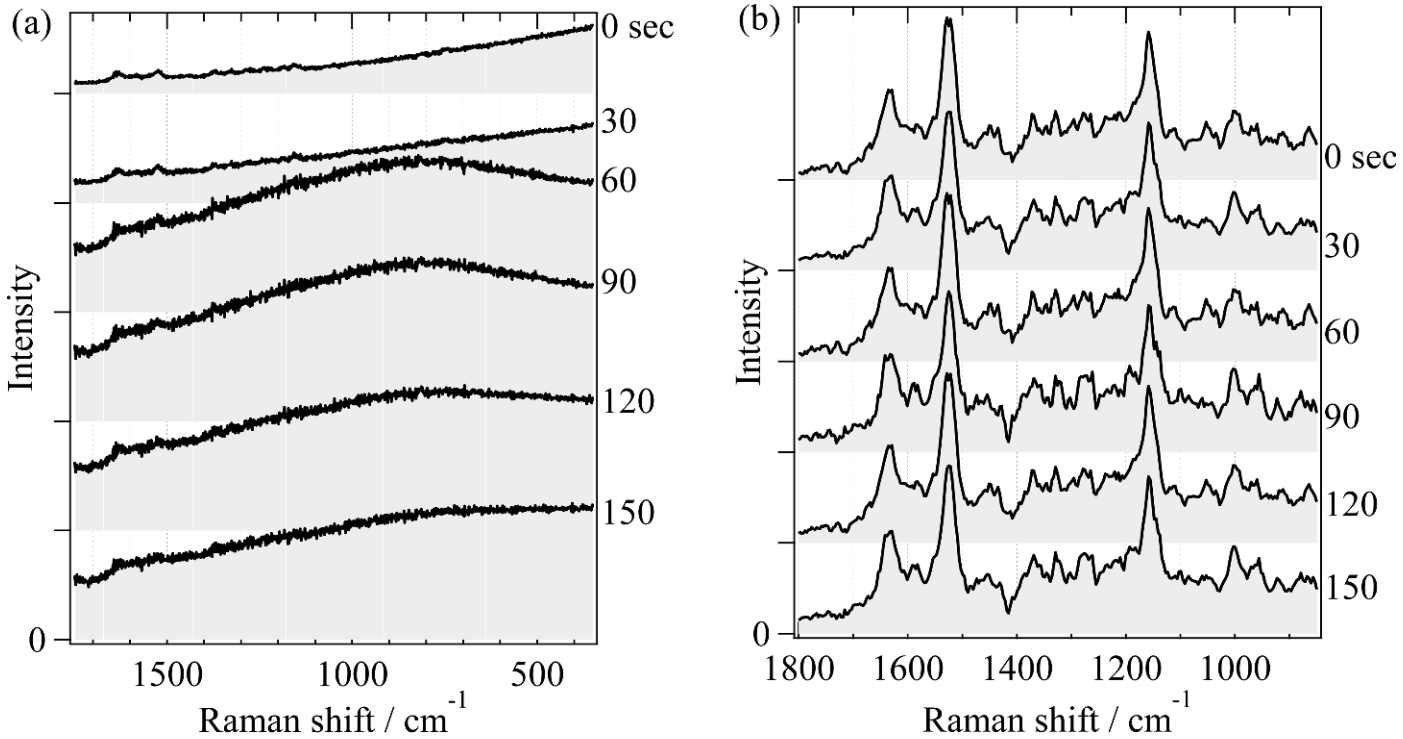

FIG. 2. (**a**) 785 nm excited and (**b**) 1064 nm excited Raman spectra of a *T. elongatus* cell with 30 s exposure and 0.6 mW laser power.

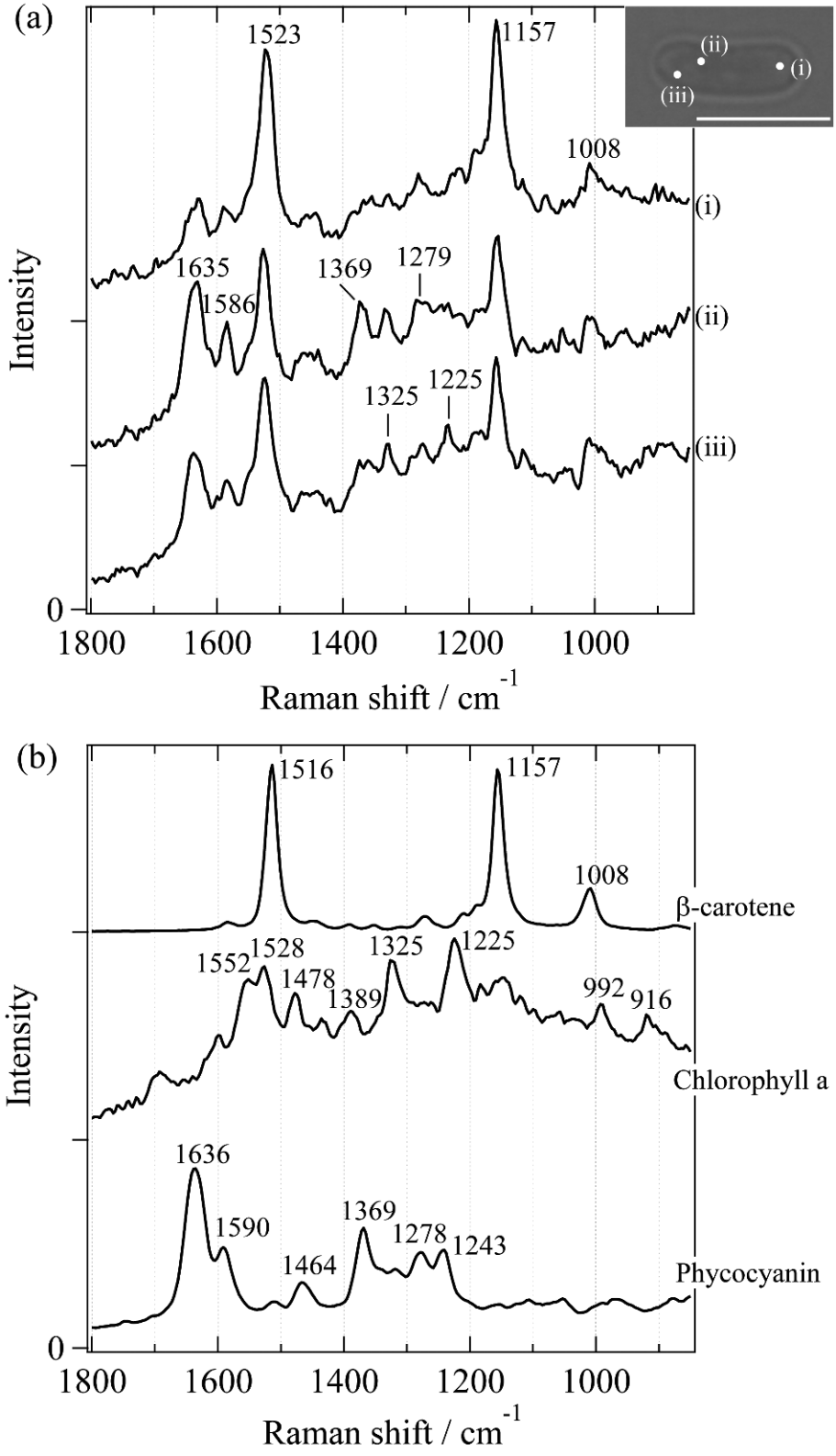

FIG. 3. (**a**) Space-resolved Raman spectra of a *T. elongatus* cell. The bar in the photograph measures 5 μm. (**b**) Raman spectra of photosynthetic pigments.

excitation is suitable for the Raman measurement of photolabile living cells.

Raman spectra measured from *T. elongatus* depend strongly on the laser focal position in the cell. Figure 3a shows space-resolved Raman spectra of a living *T. elongatus* cell obtained from three different positions as indicated in the inset. Though many Raman bands are observed in common to the three spectra, their relative intensities are quite different from one another. These Raman bands are most likely to originate from a few different molecular species having distinct distribution in

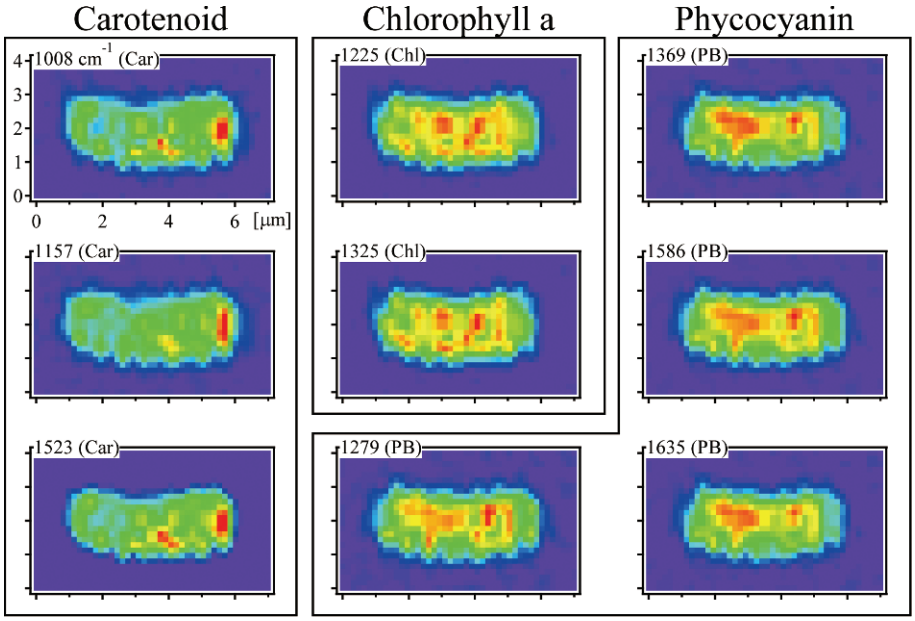

FIG. 4. Raman mapping images of each photosynthetic pigment obtained from a *T. elongatus* single living cell.

the cell. For the purpose of band assignments, Raman spectra of three photosynthetic pigments, β-carotene, chlorophyll *a*, and phycocyanin, are shown in Fig. 3b. It is readily seen from the comparison that the Raman bands at 1523, 1157, and 1008 cm^{-1} are assigned to carotenoids, i.e., the C=C stretch mode, the C–C stretch mode, and the in-plane rocking of CH_3 groups including the C–C stretch, respectively.[22] The 1635 and 1586 cm^{-1} bands are assigned to the C=C stretch mode and the in-plane N–H bending mode of phycocyanin, respectively.[23,24] Further, the bands at 1369 and 1279 cm^{-1} are also assigned to phycocyanin. The 1225 and 1325 cm^{-1} bands are assignable to chlorophyll *a* by referring to the spectrum of the model compound. In this way, the Raman spectra of *T. elongatus* are dominated by strong bands from the three photosynthetic pigments, with no distinct bands from other components such as proteins or lipids. The high intensities of these pigments most probably arise from the pre-resonance Raman effect due to their strong absorptions in the visible region.

Chemical specificity shown above enables the Raman imaging of photosynthetic pigment distributions inside a *T. elongatus* cell. Raman mapping images constructed from the band intensities at each sample point are shown in Fig. 4. These images cover a 4×7 μm area with 26×44 pixels, obtained by bicubic interpolation of the original images consisting of 13×22 pixels. The total measurement time is 3000 s. Distribution of the three photosynthetic pigments is clearly visualized in Fig. 4. Although band assignments for each pigment contain some ambiguities because of overlapping with adjacent bands, images belonging to the same pigments show the same distribution patterns. This result evidently supports the band assignments given above. It is obvious that the distributions of the three pigments are distinct from one another in the cell. In particular, carotenoids show a quite different distribution from those of chlorophyll and phycocyanin. Carotenoids are known to play several different roles in the cell, such as light harvesting, antioxidant, and photoprotection.[25–28] The unique distribution is likely to be correlated with the multifunctional nature of carotenoids in the cell. This will be a point of focus in future studies.

It is finally noted that all the spectral and imaging information is obtained with no appreciable photodamage and perturbation for the cellular processes, thanks to the deep NIR excitation. A new possibility for molecular-level and noninvasive studies of photosynthesis systems under physiological conditions is thus demonstrated.

1. G. J. Puppels, F. F. M. Demul, C. Otto, J. Greve, M. Robertnicoud, D. J. Arndtjovin, and T. M. Jovin, Nature (London) **347,** 301 (1990).
2. Y.-S. Huang, T. Karashima, M. Yamamoto, and H. Hamaguchi, Biochemistry **44,** 10009 (2005).
3. Y.-S. Huang, T. Nakatsuka, and H. Hamaguchi, Appl. Spectrosc. **61,** 1290 (2007).
4. S. E. Jorge-Villar and H. G. M. Edwards, J. Raman Spectrosc. **41,** 63 (2010).
5. C. A. Tracewell, A. Cua, D. H. Stewart, D. F. Bocian, and G. W. Brudvig, Biochemistry **40,** 193 (2001).
6. Y. K. Min, T. Yamamoto, E. Kohda, T. Ito, and H. Hamaguchi, J. Raman Spectrosc. **36,** 73 (2005).
7. M. Fujiwara, H. Hamaguchi, and M. Tasumi, Appl. Spectrosc. **40,** 137 (1986).
8. T. Hirschfeld and B. Chase, Appl. Spectrosc. **40,** 133 (1986).
9. T. Noguchi, Y. Furukawa, and M. Tasumi, Spectrochim. Acta, Part A **47,** 1431 (1991).
10. Y. Ozaki, R. Cho, K. Ikegaya, S. Muraishi, and K. Kawauchi, Appl. Spectrosc. **46,** 1503 (1992).
11. T. A. Mattioli, A. Hoffmann, D. G. Sockalingum, B. Schrader, B. Robert, and M. Lutz, Spectrochim. Acta, Part A **49,** 785 (1993).
12. H. Sato, K. Okada, K. Uehara, and Y. Ozaki, Photochem. Photobiol. **61,** 175 (1995).
13. C. Engert, V. Deckert, W. Kiefer, S. Umapathy, and H. Hamaguchi, Appl. Spectrosc. **48,** 933 (1994).
14. K. Yuzaki and H. Hamaguchi, J. Raman Spectrosc. **35,** 1013 (2004).
15. S. Kaminaka, H. Yamazaki, T. Ito, E. Kohda, and H. Hamaguchi, J. Raman Spectrosc. **32,** 139 (2001).
16. S. Kaminaka, T. Ito, H. Yamazaki, E. Kohda, and H. Hamaguchi, J. Raman Spectrosc. **33,** 498 (2002).
17. S. Naito, Y. K. Min, K. Sugata, O. Osanai, T. Kitahara, H. Hiruma, and H. Hamaguchi, Skin Res. Technol. **14,** 18 (2008).
18. T. Yamamoto, K. Yoshikiyo, Y. K. Min, H. Hamaguchi, S. Imura, S. Kudoh, T. Takahashi, and N. Yamamoto, J. Mol. Struct. **968,** 115 (2010).

19. H. G. M. Edwards, C. D. Moody, E. M. Newton, S. E. J. Villar, and M. J. Russell, Icarus **175,** 372 (2005).
20. N. Uzunbajakava, A. Lenferink, Y. Kraan, E. Volokhina, G. Vrensen, J. Greve, and C. Otto, Biophys. J. **84,** 3968 (2003).
21. M. Sugiura and Y. Inoue, Plant Cell Physiol. **40,** 1219 (1999).
22. S. Saito and M. Tasumi, J. Raman Spectrosc. **14,** 310 (1983).
23. C. Kneip, A. Parbel, H. Foerstendorf, H. Scheer, F. Siebert, and P. Hildebrandt, J. Raman Spectrosc. **29,** 939 (1998).
24. C. Kneip, P. Hildebrandt, K. Nemeth, F. Mark, and K. Schaffner, Chem. Phys. Lett. **311,** 479 (1999).
25. S. Steiger, L. Schafer, and G. Sandmann, J. Photochem. Photobiol. B-Biol. **52,** 14 (1999).
26. A. Wilson, G. Ajlani, J. M. Verbavatz, I. Vass, C. A. Kerfeld, and D. Kirilovsky, Plant Cell **18,** 992 (2006).
27. D. Kirilovsky, Photosynth. Res. **93,** 7 (2007).
28. S. Bailey and A. Grossman, Photochem. Photobiol. **84,** 1410 (2008).